INTERNATIONAL JOURNAL OF INTEGRATED ENGINEERING
ISSN: 2229-838X e-ISSN: 2600-7916

IJIE

Vol. 17 No. 5 (2025) 187-201
https://publisher.uthm.edu.my/ojs/index.php/ijie

Dynamic Properties of Pot Bearing Via Modal Analysis

Ahmad Idzwan Yusuf[1]*, Norliyati Mohd Amin[1], Mohd Azmi Yunus[2], Norrul Azmi Yahya[1]

[1] *Faculty of Civil Engineering, Universiti Teknologi MARA, Selangor, 40450, MALAYSIA*
[2] *Faculty of Mechanical Engineering, Universiti Teknologi MARA, Selangor, 40450, MALASYIA*

*Corresponding Author: ahmadidzwan@uitm.edu.my
DOI: https://doi.org/10.30880/ijie.2025.17.05.015

Article Info

Received: 27 November 2023
Accepted: 29 July 2025
Available online: 30 August 2025

Keywords

Pot bearing, finite element modal analysis, experimental modal analysis, dynamic analysis

Abstract

Bearings represent one of the most sensitive and demanding elements in load transfer, particularly in structural support systems, which have some of the highest requirements regarding reliability and performance in structural engineering. One widely used structural bearing is the mechanical pot bearing. This compact bearing is especially useful for transmitting large vertical loads while accommodating extensive movements and multi-directional rotation. Understanding the dynamic behavior of the pot bearing in terms of natural frequencies, mode shapes, and damping is a necessity for enhancing its design and failure limit. Since it is composed of several materials, the pot bearing exhibits complex material behavior, making the measurement of its dynamic properties challenging in real practice. Modal analysis is one of the best methods used to determine the dynamic properties of materials. Consequently, the main objective of this research is to determine the dynamic properties of the pot bearing, specifically natural frequencies, mode shapes, and damping, through numerical modeling and experimental work based on modal analysis. From the findings, the relative errors between the finite element and experimental modal analyses for the first mode are quantified at 15.29%, whereas for the second mode, the corresponding value is 10.13%. The third mode demonstrates a relative error of 9.67%, while the fourth mode exhibits the lowest relative error of 8.81%. A strong agreement in mode shape was observed between the finite element model and experimental modal analysis results. In conclusion, modal analysis proved to be an effective technique for capturing the dynamic characteristics of pot bearings. The validated numerical model offers a reliable basis for further analysis, optimization, and integration into broader structural dynamic assessments.

1. Introduction

Seismic isolation bearings have been extensively employed in engineering applications due to their effectiveness in mitigating the effects of seismic events on structures [1]–[5]. Isolation systems can be divided into three different categories: sliding isolation bearings, which include pendulum and pot bearings; spring-like isolation bearings, which include laminated and lead rubber bearings; and hybrid systems, which combine features from both of the aforementioned bearing types [6]. Through their distinct energy dissipation mechanisms, each of these bearings has the ability to lessen the transfer of inertia forces to the structure and dissipate seismic energy. Due

This is an open access article under the CC BY-NC-SA 4.0 license.

to their affordability and simplicity of use, sliding isolation bearings in particular are frequently used in construction projects [7]–[9].

Among various types of bearings, pot bearings are extensively used in bridges due to their ability to support high vertical loads and accommodate rotational and translational movements. A pot bearing is a cutting-edge sliding isolation bearing made of PTFE (polytetrafluoroethylene), rubber, and steel. In comparison to other structural bearings, it has benefits such as a higher bearing capacity, more horizontal displacement, flexible rotation, and a longer service life of up to 25 years. This bearing also requires little maintenance and is fully detachable and simple to install. The elastomer pad and PTFE are important synthetic materials used in pot bearings. The rubber-based elastomer pad, which provides translation and rotation without the use of moving parts and displays fluid-like behaviour at high pressures, enables higher working pressures in smaller spaces. Low coefficient of friction and exceptional resistance to wear, impact, and ageing are two characteristics of PTFE. Pot bearings are made to withstand a variety of vertical and horizontal loads, as well as rotation and lateral, longitudinal, and lateral movements [10].

Due to their deformability, pot bearings can rotate around any axis and support heavy loads of up to 50,000 kN. These bearings use different rotational and translational mechanisms, resulting in minimal load eccentricity and frictional movement resistance. The absence of compressive deflection, fluid-like behaviour under high pressure, rotational movement made possible by shear deformation of the encased elastomeric rubber pad, and prevention of rubber bulging due to the pot walls are a few of the major benefits. They are especially well suited for medium to long-span structures like bridges, pipelines, power plants, and offshore platforms because of their design characteristics. Pot bearings are the subject of ongoing research and development with the goal of achieving simplicity, design efficiency, versatility, and cost effectiveness [11].

Pot bearings are important, which has motivated researchers to investigate their behaviour and improve their design. Designing a successful base isolation system requires a thorough understanding of isolator characteristics [12]. Engineering foundations, superstructures, and substructures of bridges have been the subject of extensive research in recent years [13]. However, despite the fact that bearing failure can lead to the collapse of entire bridges or other structures, as well as the failure of bridge piers and abutments, comprehensive research on bearings has been relatively limited [14].

The majority of bearings-related studies [15], [16] focus primarily on how bearings behave during seismic events. In the past, to represent bearing movements between girders and piers, researchers frequently used streamlined spring elements in analytical models [16]. Such streamlined elements, however, are unable to faithfully reproduce the sliding and frictional behaviour seen in real bearing structures. As a result, earlier models neglected to take into account crucial bearing failure modes like slippage or displacement from their initial positions [17]. The impact of vertical and horizontal loads on bearing stability [18]–[20], the impact of shape factors on mechanical properties [21], [22], the effects of temperature on bearings [23], the buckling load capacity [24], and the instability of bearings brought on by cavitation [25] are a few other topics that have been the subject of research in this area.

Resonance may happen when a structure is exposed to external dynamic loads, such as earthquakes or other forces that are close to its natural frequency. This can cause structural damage and even collapse. This situation also applies to pot bearings because resonance can happen when they encounter external dynamic loads that are close to their natural frequencies, leading to structural failure and bearing damage. According to surveys of the damage caused by the earthquake, many failures are caused by defective bearings [26].

Understanding pot bearings' dynamic properties is crucial because they are essential for protecting structures from outside dynamic loads. To the best of the authors' knowledge, no studies have evaluated the pot bearings' dynamic characteristics. Designing efficient base isolation systems that can avoid bearing resonance is made possible by an understanding of these properties [27], [28]. In order to determine the dynamic characteristics of mechanical pot bearings, specifically their natural frequencies, mode shapes, and damping, further study is required.

2. Modal Analysis

A technique called modal analysis is used to determine a system's natural frequencies, mode shapes, and damping [29]. These dynamic characteristics enable modifications or improvements to the system's design and a deeper understanding of the behaviour of the system. The system will oscillate at one of its natural frequencies under the right initial conditions, producing mode shapes as it does so. Both theoretical and experimental methods are used in modal analysis [29], [30]. Dynamic properties are determined in theoretical modal analysis using analytical or numerical techniques like formulation or finite element analysis. On the other hand, experimental modal analysis uses the real physical system and field measurements to identify dynamic properties.

Int. Journal of Integrated Engineering Vol. 17 No. 5 (2025) p. 187-201

2.1 Experimental Modal Analysis

A common technique used by modal analysts to ascertain dynamic behaviour, operational circumstances, and performance criteria is experimental modal analysis (EMA). These factors support the design of the best dynamic behaviour or the correction of structural dynamic problems in existing designs. In this method, a structure is stimulated, and the response's acceleration, velocity, and displacement are then measured. The Fourier transform is used to transform the signal produced by excitation and response into the frequency domain, which results in the acquisition of frequency functions, also referred to as transfer functions. The frequency response function (FRF) is a sophisticated mathematical function that results from the Fourier transform [31]. As a component of non-destructive testing [32], EMA is practical and cost-effective.

Test setup, FRF measurements, and the identification of dynamic behaviour (natural frequencies, mode shapes, and damping) make up the three stages of EMA. The selection of force and vibration transducers, recording methods, excitation strategies, excitation sites, hardware, and measurement locations are all part of the test preparation process [33]–[35]. A set of FRF data is collected and stored during the testing phase for later analysis to ascertain the dynamic behaviour of the tested structure. The quick and precise analysis of a structure's dynamic behaviour is made possible by EMA. The accuracy of the measured FRF has a significant impact on the quality of EMA results. Therefore, it is essential for EMA to evaluate the level of the measured FRF. The relationship between the FRF's output response and input signal can be expressed as follows:

$$F(\omega) + [H(\omega)] = X(\omega) \tag{1}$$

and

$$[H(\omega)] = X(\omega) / F(\omega) \tag{2}$$

Where F (ω) is the input signal, X (ω) is the output response, and H (ω) represents the dynamic properties of the structure.

2.2 Experimental Modal Analysis

A type of analysis used with the finite element method is finite element modal analysis. It is used to determine the natural frequencies and mode shapes of different materials or structures. The mode shapes that are represented by the system's displacements are referred to as eigenvectors, and the natural frequencies of a system are also known as eigenvalues. External excitation and damping are ignored in this modal analysis. In the case of free vibration, the equation of motion for a single degree of freedom (SDoF) system can be written as follows [30]:

$$[\mathbf{M}]\{\ddot{x}\} + [\mathbf{K}]\{x\} = \{0\} \tag{3}$$

Free vibration solution is mathematically non trivial solution. It should take the form as:

$$\{x\} = \{X\} \sin \omega t \tag{4}$$

By substituting Equation (4) into Equation (2), a simple algebraic matrix equation can be expressed as below:

$$([\mathbf{K}] - \omega 2\,[\mathbf{M}])\,\{X\} = \{0\} \tag{5}$$

In Equation (5), {X} cannot be 0, so:

$$|[\mathbf{K}] - \omega 2[\mathbf{M}]| = \{0\} \tag{6}$$

In this expression, [K] and [M] represent the stiffness and mass matrices of the system, respectively. The eigenvalue, denoted by ω2, establishes the system's natural frequency, while the eigenvector, symbolised by {X}, determines the system's mode shape.

3. Methodology

The modal analysis method was used in this study to determine the pot bearings' dynamic properties. Both numerical and experimental methods can be used in modal analysis. The experimental modal analysis used impact hammer testing, whereas the numerical modal analysis used the finite element programme ANSYS. Both methods' outputs for mode shapes and natural frequencies were compared and verified. Since damping is taken into account

in experimental modal analysis but not in finite element modal analysis, natural frequency values from the finite element analysis are typically anticipated to be higher than those from the experiment. The dissipation of energy within the material is referred to as damping.

3.1 Materials

This study focused on one mechanical pot bearing. The pot bearing is made up of a number of components, including an upper steel plate, sliding PTFE, a piston, an elastomeric rubber pad, a bottom bolt, and a bottom plate. Table 1 lists the components and measurements used for the pot bearing. The typical drawings and the actual pot bearing used in this study are shown in Fig. 1 and 2.

Table 1 *Material and dimensions used for pot bearing*

Material	Dimension
Top Slide Plate	370 x 420 x 20 mm
Mating Surface	280 x 410 x 1.5 mm
Sliding PTFE Surface	ϕ 200 x 5 mm
Piston	ϕ 219 x 20 mm
Elastomer Rubber Pad	ϕ 220 x 12 mm
Cylinder	ϕ 260 x 34 mm
Bottom Attachment Plate	370 x 270 x 10 mm
Bottom Attachment Bolt	M16 x 60 mm, Grade 8.8

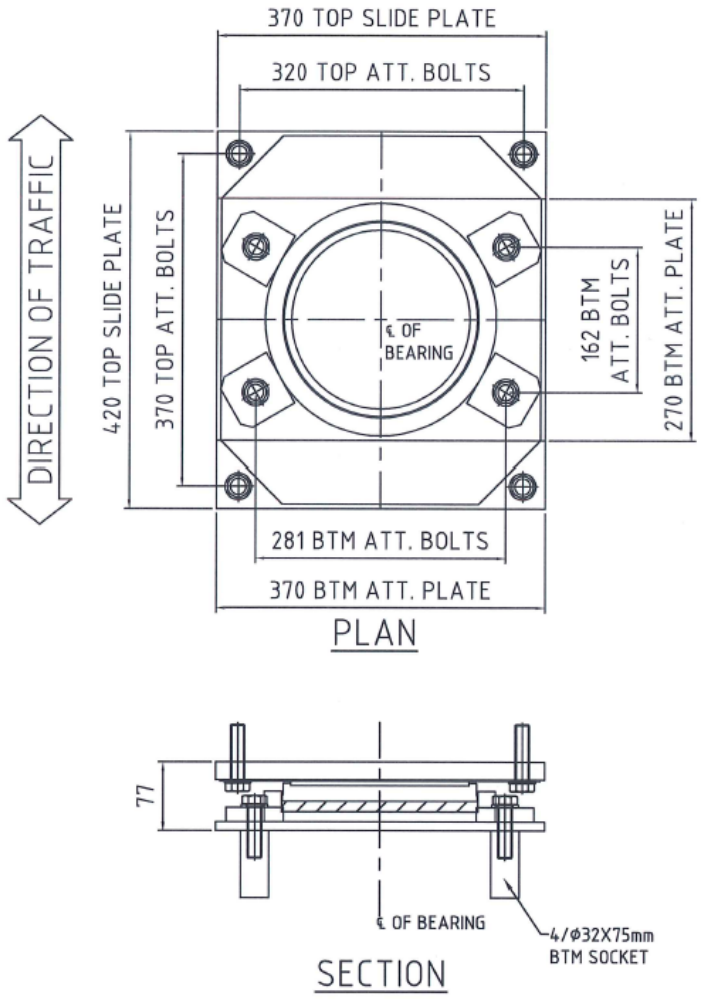

Fig. 1 *Typical drawing of pot bearing*

Int. Journal of Integrated Engineering Vol. 17 No. 5 (2025) p. 187-201

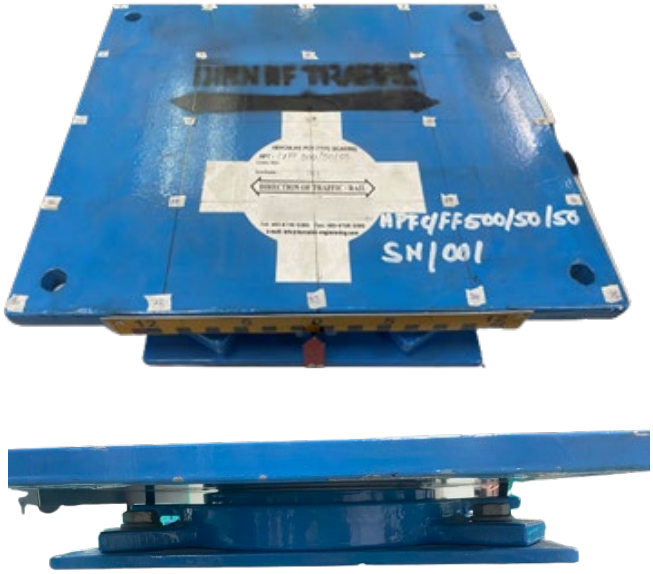

Fig. 2 *Actual pot bearing*

3.2 Finite Element Modal Analysis

The pot bearing was modelled and examined using ANSYS for the finite element modal analysis. The geometry modelling of the pot bearing was initially done using AutoCAD due to the bearing's complexity. The geometry was subsequently exported to ANSYS for analysis. The geometry modelling of the pot bearing using AutoCAD is shown in Fig. 3 and 4. Each material in the pot bearing was given particular material properties within ANSYS. Modelling the pot bearing as closely as possible to the real physical pot bearing is essential. The material properties used in the modelling of this bearing are shown in Table 2. The manufacturer of the pot bearing provided the material properties. A mesh size of 10 mm was employed for the purpose of meshing the pot bearing. Regarding boundary conditions, the pot bearing was affixed at the base of the pot bearing's bolt, resembling the experimental modal analysis in which the bearing was fixed at the lowermost part. Fig. 5 depicts the meshed pot bearing utilised in the finite element modal analysis.

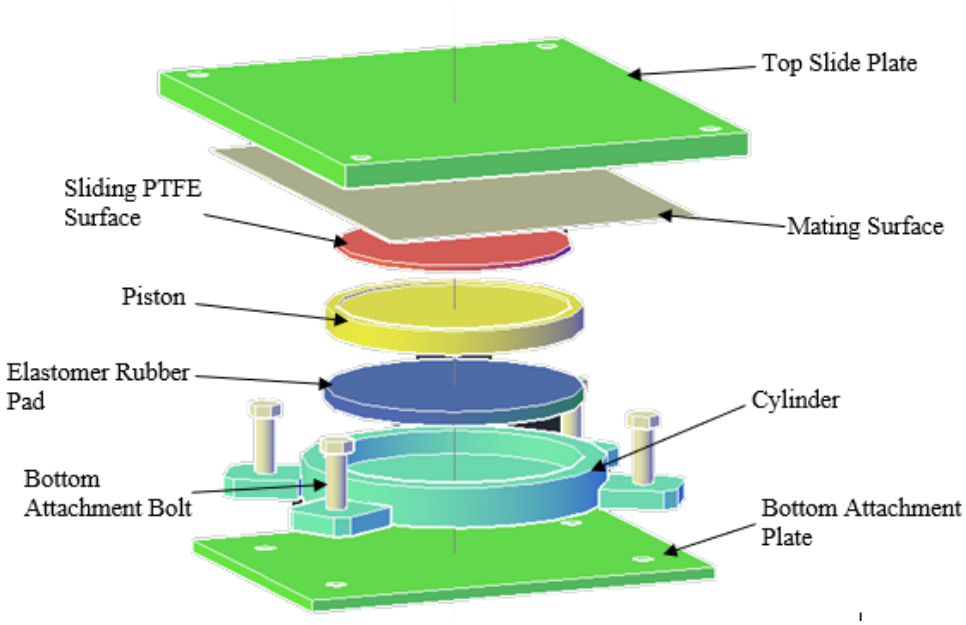

Fig. 3 *Assemble geometry of pot bearing in AutoCAD*

.

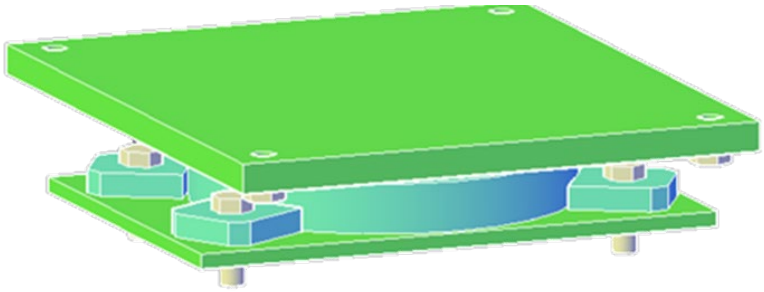

Fig. 4 *Geometry of pot bearing in AutoCAD*

Table 2 *Material properties for pot bearing*

Materials	Young's Modulus	Poisson's Ratio	Density (kg/m^3)
Steel	200GPa	0.3	7850
Natural Rubber	50MPa	0.49	1100
Stainless Steel 316	193GPa	0.265	8000
Polytetrafluoroethylene (PTFE)	400MPa	0.46	2300

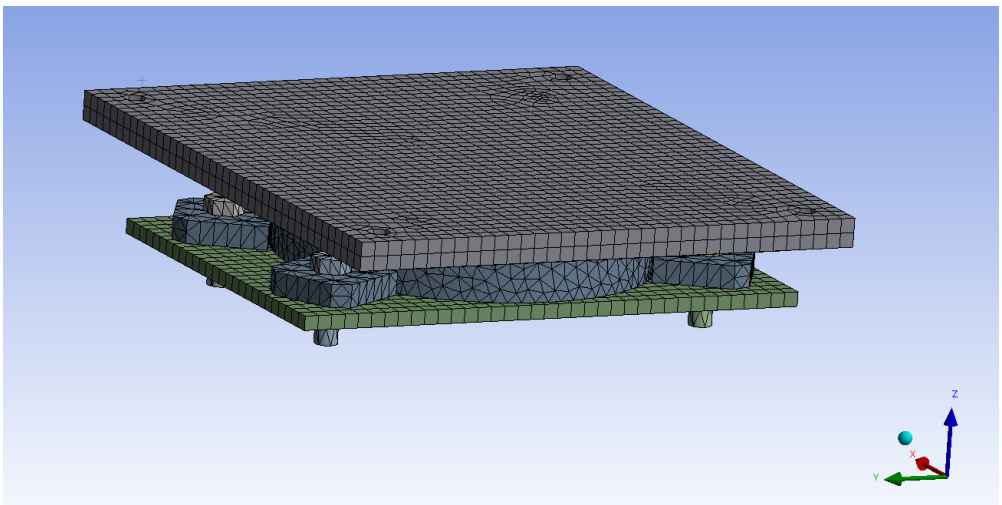

Fig. 5 *Meshed pot type model*

Following this, the pot bearing was subjected to analysis, and the findings pertaining to its natural frequencies and mode shapes were extracted. Subsequently, a comparison was made between the aforementioned results and the data derived from the experimental modal analysis.

3.3 Experimental Modal Analysis

In the context of Experimental Modal Analysis (EMA), the necessary components for conducting the analysis consist of force transducers, vibration transducers, an acquisition system, and software. The force transducer is used to measure the excitation force, while the motion transducer is employed to measure the corresponding signal. In general, the input signal of the system is commonly denoted as the excitation force, which is quantified

Int. Journal of Integrated Engineering Vol. 17 No. 5 (2025) p. 187-201

through the utilisation of a force transducer for measurement purposes. For the purpose of this experiment, a printed circuit board (PCB) impact hammer with a sensitivity of 11.76 millivolts per gramme (mV/g) was utilised for stimulation. The resultant signal generated by the vibrating structure generally encompasses accelerations, velocities, and displacements measured at different locations on the structure. The measurement of these system outputs is typically conducted using a motion transducer called an accelerometer. The careful selection of an appropriate accelerometer is of utmost importance in certain scenarios, taking into account various factors including the frequency range, sensitivity, and weight of the device. In this particular case study, the researchers utilised three single-axis Dytran accelerometers to assess the response at specific points of interest along the X, Y, and Z axes.

Following this, frequency response functions (FRFs) and vibration data obtained from the structure can be measured, recorded, and processed utilising data acquisition equipment. When choosing an acquisition system, it is important to take into account various factors. These factors include the quantity of measurement channels, the maximum frequency bandwidth, the level of accuracy, the overall speed and performance, and the compatibility with existing hardware and software. There exist multiple categories of acquisition systems, encompassing PC-based systems, FFT analyzers integrated with PCs or workstations, and acquisition front-ends coupled with workstations. The acquisition front-end, when paired with a workstation, is widely favoured in various applications due to its exceptional versatility and robust capabilities. The vibration data analysis in this study utilised a Siemens LMS SCADAS analyzer front-end equipped with 16 channels.

The structural integrity of a test must be upheld through appropriate support from its surrounding environment. The application of boundary conditions to the test structure, such as fixed support or hinges, may seem simpler in theory. In this study, the experimental modal analysis (EMA) was performed on the test structures using a setup that implemented fixed boundary conditions at the base of the pot bearing. The test configuration closely resembles the finite element model, wherein fixed boundary conditions were applied at the base of the model.

Initially, the pot bearing was divided into 25 measurement points prior to conducting EMA, as depicted in Fig. 6. The selection of measurement points was based on the mode shapes observed from the finite element model of the pot bearing. Prior to conducting experimental modal analysis, it is imperative to possess a fundamental comprehension of the mode shapes and frequency bandwidth of the structure. The dynamic behaviour of the structure can be determined by employing finite element analysis as an initial step. Put simply, the outcomes of finite element analysis can provide valuable insights for conducting experimental investigations on real structures. The selection of excitation and measurement points in the test was based on the finite element results, aiming to ensure that all modes of interest could be accurately measured. It is imperative to ensure that the measurement points are evenly distributed throughout the structure being examined. This approach decreases the probability of overlooking a mode and enhances the coherence of the animated mode visualisation in the experiment. Moreover, the positioning of the accelerometers plays a crucial role in determining the precision of the test outcomes and the extent of the frequency spectrum examined.

The experiment involved the utilisation of a mobile hammer to perform tests. The hammer was used to apply excitation at each of the 25 measurement locations along the vertical axis of the pot bearing. The first measurement point served as the reference point for the experiment. The structure underwent three excitations at each measurement point, with each measurement utilising the identical trigger level as the excitation caused by the impact hammer. In order to collect the dynamic data, three uniaxial accelerometers with a sensitivity of 10 mV/g were attached to measurement point 1 along the X, Y, and Z axes, as illustrated in Fig. 7. The researchers employed the Siemens Leuven Measurement System (LMS) SCADAS analyzer to gather all the Frequency Response Function (FRF) data. A frequency bandwidth ranging from 0 Hz to 2000 Hz was defined, with a frequency resolution of 1 Hz. The process of curve fitting and mode selection was conducted utilising the Polymax method, as described in reference [29]. The EMA configuration for the pot bearing, which is affixed at the base of the bearing, is depicted in Fig. 8. The experimental setup adhered to the ISO 7626-5:2019 standard Mechanical Vibration and Shock – Experimental Determination of Mechanical Mobility Part 5 ensuring the experiment's compliance with best practices for modal testing.

Fig. 6 *Marked pot bearing*

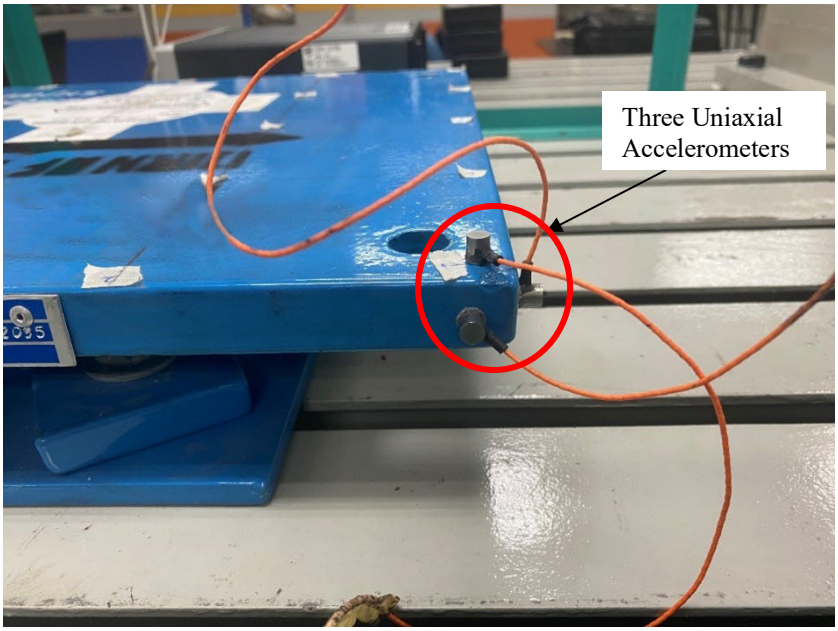

Fig. 7 *Three uniaxial accelerometers in X, Y and Z direction*

Int. Journal of Integrated Engineering Vol. 17 No. 5 (2025) p. 187-201

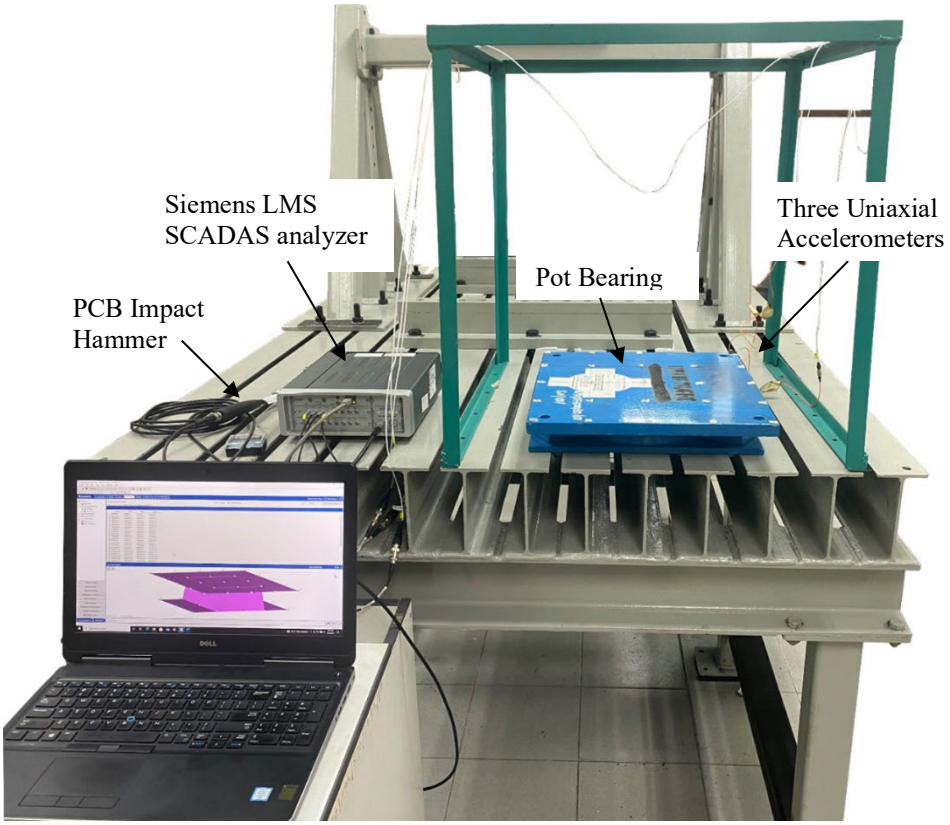

Fig. 8 *EMA setup for pot bearing*

4. Results and Discussion

Table 3 presents the relationship between different natural frequencies and the corresponding mode shapes exhibited by the pot bearing that were extracted from the finite element modal analysis. The initial bending deformation pattern of the mode shape was produced by mode F1, which possesses a natural frequency of 566.16 Hz. In contrast, the subsequent bending deformation pattern of the mode shape was generated by mode F2, exhibiting a natural frequency of 920.17 Hz. In mode F3, the initial torsion mode shape was produced, exhibiting a natural frequency of 1259.10 Hz. The second mode shape of torsion was generated for mode F4, exhibiting a natural frequency of 1236.60 Hz. Damping values are not included in the analysis of the finite element modal system, as it is assumed to be a free vibration system according to equation (3). Damping pertains to the dissipation of energy or the occurrence of energy losses within a vibrational system. The frequency response function (FRF) of the pot bearing obtained from the experimental modal analysis is depicted in Fig. 9. Table 4 presents a comprehensive overview of the outcomes pertaining to the natural frequencies and mode shapes of the pot bearing. These results were obtained through the extraction process from the frequency response function (FRF) during the experimental modal analysis.

Table 3 *Finite element modal analysis for pot bearing*

Mode No.	Natural Frequencies (Hz)	Mode Shape	Mode Shape Description
F1	566.16 Hz	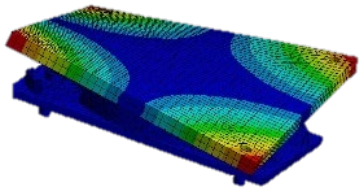	1st bending
F2	920.17 Hz	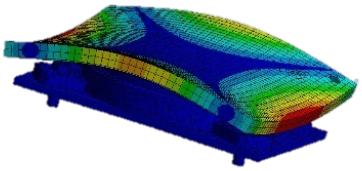	2nd bending
F3	1259.10 Hz	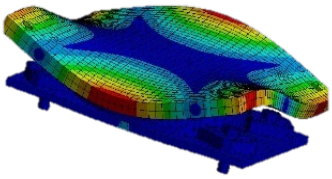	1st Torsion
F4	1293.60 Hz	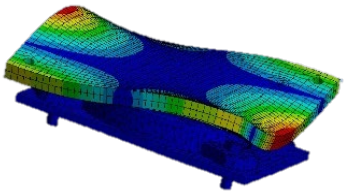	2nd Torsion

Int. Journal of Integrated Engineering Vol. 17 No. 5 (2025) p. 187-201

Table 4 *Experimental modal analysis for pot bearing*

Mode No.	Natural Frequency [Hz]	Damping Ratio (%)	Mode Shape	Mode Shape Description
E1	491.51	2.52	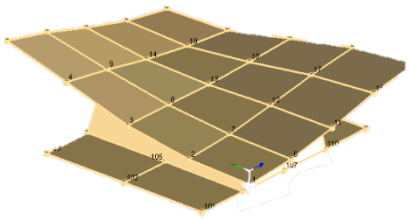	1st bending
E2	835.55	2.01	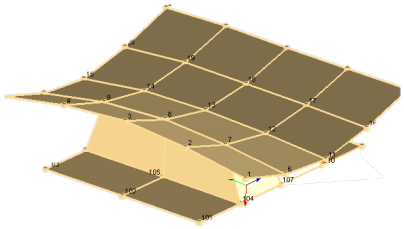	2nd bending
E3	1148.10	2.02	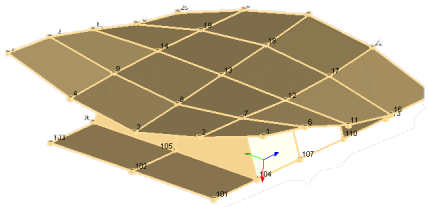	1st Torsion
E4	1188.88	0.59	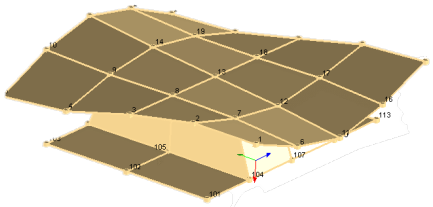	2nd Torsion

Table 4 displays four modes that have been extracted from the FRF of the pot bearing. The initial mode exhibits a fundamental frequency of 491.51 Hz and a damping ratio of 2.52%. Consequently, it manifests a mode shape that corresponds to the first bending deformation pattern. The second mode exhibits a natural frequency of 835.55 Hz and manifests bending deformation patterns characterised by mode shapes. These mode shapes are accompanied by a damping ratio value of 2.01%. Modes three and four produce the initial and secondary torsional deformation configurations of mode shapes, exhibiting natural frequencies of 1148.10 Hz and 1188.88 Hz, correspondingly. The damping ratios associated with modes three and four were determined to be 2.02% and 0.59%, respectively.

Upon comparing Tables 3 and 4, it is evident that there is a notable concurrence in the mode shapes between the finite element and experimental modal analyses across all four modes. A total of four modes have been effectively derived from the experimental modal analysis, demonstrating favourable outcomes in comparison to the finite element modal analysis. This can be attributed to the intricate nature of the pot bearing. Table 5 presents a comparative analysis of the mode shapes obtained from the finite element and experimental modal analyses.

Meanwhile, Table 6 illustrates the relative error in the natural frequencies of the pot bearing when comparing the results obtained from both methods.

Table 5 *Mode shape comparison between finite element and experimental modal analysis*

Mode No.	Finite Element	Experiment	Mode Shape Description
1	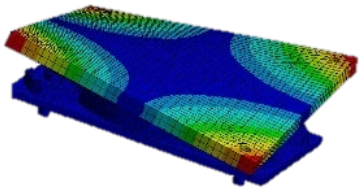	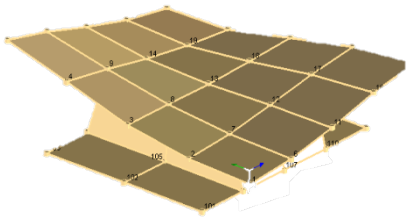	1st bending
2	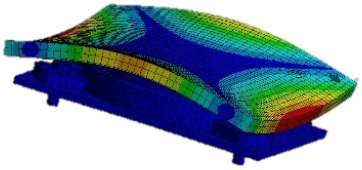	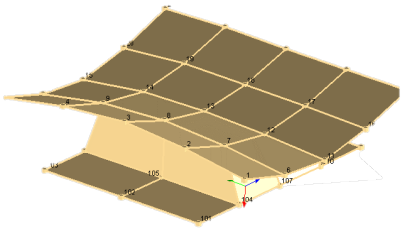	2nd bending
3	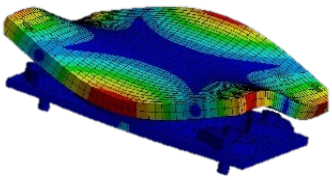	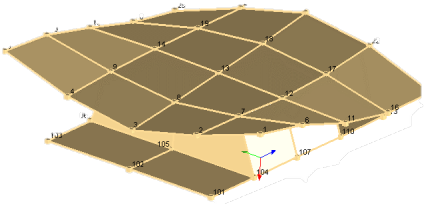	1st Torsion
4	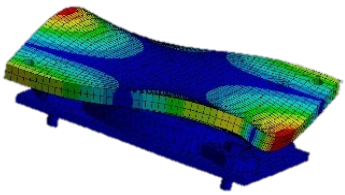	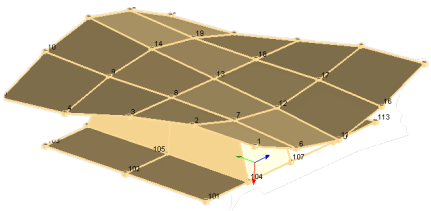	2nd Torsion

Int. Journal of Integrated Engineering Vol. 17 No. 5 (2025) p. 187-201

Table 6 *Relative error between finite element and experiment*

Mode No.	Finite Element [Hz]	Mode No.	Experimental [Hz]	Relative Error [%]
F1	566.16	E1	491.51	15.29
F2	920.17	E2	835.55	10.13
F3	1259.10	E3	1148.10	9.67
F4	1293.60	E4	1188.88	8.81

The findings presented in Table 6 indicate that the natural frequencies derived from the finite element analysis and the experimental modal analysis of the pot bearing exhibit negligible disparities across all modes. The relative errors between the finite element and experimental modal analyses for modes F1 and E1 are quantified at 15.29%, whereas for modes F2 and E2, the corresponding value is 10.13%. Modes F3 and E3 demonstrate a relative error of 9.67%, while modes F4 and E4 exhibit the lowest relative error of 8.81%. It is important to note that the initial finite element modal analysis (FEMA) did not incorporate damping effects, which inherently influence the system's stiffness and dynamic response. As a result, the computed natural frequencies from the finite element model were slightly higher than those observed experimentally. This discrepancy highlights the need for model updating and optimization to enhance the accuracy of the numerical prediction and better reflect the actual dynamic behavior of the pot bearing analysis. The findings of this study suggest that in the process of designing or evaluating a structure, it is imperative to take into account the vibrational characteristics of the pot bearing, as it has a significant influence on the overall stability of the structure [11].

5. Conclusion

The dynamic characteristics of pot bearings have been effectively assessed through modal analysis using both finite element simulations and experimental testing. The integration of these two approaches enabled accurate identification of natural frequencies and corresponding mode shapes, providing a comprehensive understanding of the bearing's vibrational behavior. Four significant modes were successfully captured, with strong agreement observed between the predicted mode shapes from the finite element model and those obtained experimentally. However, notable discrepancies were identified in the natural frequencies across all modes. The highest relative error was recorded for the first mode at 15.29%, followed by 10.13% for the second mode, 9.67% for the third, and 8.81% for the fourth. These differences emphasize the necessity for model updating and optimization to improve the correlation between numerical predictions and experimental observations. By refining key material and structural parameters, the updated model can more accurately reflect the real dynamic behavior of pot bearings.

This enhanced and validated finite element model serves as a robust foundation for further analysis, particularly in harmonic response evaluations, where accurate dynamic representation is crucial. Overall, the findings underscore the value of integrating numerical and experimental techniques in characterizing complex structural components and improving the fidelity of dynamic performance assessments in civil engineering applications

Acknowledgement

The authors would like to express their sincere gratitude to Universiti Teknologi MARA, Dr. Wan Imaan Izhan Bin Wan Iskandar Mirza, and the Structural Dynamics Analysis & Validation (SDAV) team at the College of Engineering, UiTM Shah Alam. Their invaluable support, insights, and contributions were instrumental to the success of this work and are deeply appreciated.

Conflict of Interest

Authors declare that there is no conflict of interests regarding the publication of the paper.

Author Contribution

The authors confirm contribution to the paper as follows: ***study conception and design****: Ahmad Idzwan Yusuf, Norliyati Mohd Amin;* ***data collection****: Ahmad Idzwan Yusuf, Mohd Azmi Yunus;* ***analysis and interpretation of results****: Ahmad Idzwan Yusuf, Norrul Azmi Yahya, Mohd Azmi Yunus;* ***draft manuscript preparation****: Ahmad Idzwan Yusuf, Norliyati Mohd Amin. All authors reviewed the results and approved the final version of the manuscript.*

References

[1] Xiang, N. & Alam, M.S. (2019) Comparative seismic fragility assessment of an existing isolated continuous bridge retrofitted with different energy dissipation devices, *Journal of Bridge Engineering*, *24(8)*, 04019070, https://doi.org/10.1061/(ASCE)BE.1943-5592.0001425

[2] Xiang, N. & Alam, M.S. (2019) Displacement-based seismic design of bridge bents retrofitted with various bracing devices and their seismic fragility assessment under near-fault and far-field ground motions, *Soil Dynamics and Earthquake Engineering*, *119*, 75–90, https://doi.org/10.1016/j.soildyn.2018.12.023

[3] Li, S., Dezfuli, F.H.,Wang, J. & Alam, M.S. (2020) Seismic vulnerability and loss assessment of an isolated simply-supported highway bridge retrofitted with optimized superelastic shape memory alloy cable restrainers, *Bulletin of Earthquake Engineering*, *18*, 3285–3316, https://doi.org/10.1007/s10518-020-00812-4

[4] Cao, S., Ozbulut, O.E., Shi, F. & Deng, J. (2022) An SMA cable-based negative stiffness seismic isolator: Development, experimental characterization, and numerical modeling, *Journal of Intelligent Material Systems and Structures*, 33, 1819–1833, https://doi.org/10.1177/1045389X21107221

[5] Chen, X., Ikago, K., Guan, Z., Li, J. & Wang, X. (2022) Lead-Rubber-Bearing with Negative Stiffness Springs (LRB-NS) for Base-Isolation Seismic Design of Resilient Bridges: A Theoretical Feasibility Study, *Engineering Structures*, *266*, 114601, https://doi.org/10.1016/j.engstruct.2022.114601

[6] Chakraborty, S., Roy, K. & Ray-Chaudhuri, S. (2016) Design of re-centering spring for flat sliding base isolation system: Theory and a numerical study, *Engineering Structures*, *126*, 66–77, https://doi.org/10.1016/j.engstruct.2016.07.049

[7] Yin, P., Wang, J., & Pang, Y. (2022) Seismic Performance of a Sliding Isolation Bridge System with a New Spring Re-Centering Device, *Sustainability 2022*, *14(17)*, 10720, https://doi.org/10.3390/su141710720

[8] Li, S., Wang, J. & Alam, M. S. (2021) Seismic performance assessment of a multispan continuous isolated highway bridge with superelastic shape memory alloy reinforced piers and restraining devices, *Earthquake Engineering & Structural Dynamics*, *50*, 673–691, https://doi.org/10.1002/eqe.3353

[9] Yi, J., Zhou, J. & Ye, X. (2022) Seismic control of cable-stayed bridge using negative stiffness device and fluid viscous damper under near-field ground motions, *Journal of Earthquake Engineering*, *26*, 2642–2659, https://doi.org/10.1080/13632469.2020.1785588

[10] Shiau, Y. C., Wang, M. T., Huang, C. M., & Zeng, J. Y. (2008) Discussion of pot bearing for concrete bridge, *ISARC 2008 - Proceedings from the 25th International Symposium on Automation and Robotics in Construction*, 213–223, https://doi.org/10.3846/isarc.20080626.213

[11] Arunkiliyal, R, Abinaya, S., Divya, R., Suganthi, K. & Sridar, M. (2017) Comparative Study on Bridge Pot bearing by using ANSYS and SAP2000 Software, *International Journal of Innovative Research in Science, Engineering and Technology*, *6(5)*, 9724–9730, https://doi.org/10.15680/IJIRSET.2017.0605311

[12] Yusuf, A. I., & Amin, N. M. (2019) Rayleigh Damping Coefficients of Laminated Rubber Bearing, *International Journal of Recent Technology and Engineering*, *8(4)*, 12294–12300, https://doi.org/10.35940/ijrte.d5203.118419

[13] Wang, W., Li, C., Rens, K. L., & Nogueira, C. L. (2020) Failure Analysis of Pot Bearings in a Curved Viaduct, *Journal of Performance of Constructed Facilities*, *34(5)*, 1–9, https://doi.org/10.1061/(asce)cf.1943-5509.0001463

[14] Wang, R. Z., Chen, S. K., Liu, K. Y., Wang, C. Y., Chang, K. C. & Chen, S. H. (2014) Analytical simulations of the steel-laminated elastomeric bridge bearing, *Journal of Mechanics*, *30(4)*, 373–382, https://doi.org/10.1017/jmech.2014.24

[15] Fan, X. & McCormick, J. P. (2014) Characterization of the behavior of steel bridge bearings under cyclic load reversal, *Structure and Infrastructure Engineering*, *11(6)*, 744–760, https://doi.org/10.1080/15732479.2014.905963

[16] Li, X., Zhang, Z. & Zhang, X. (2016) Using elastic bridge bearings to reduce train-induced ground vibrations: An experimental and numerical study, *Soil Dynamics and Earthquake Engineering*, *85*, 78–90, https://doi.org/10.1016/j.soildyn.2016.03.013

[17] McDonald, J., Heymsfield, E. & Avent, R. R. (2000) Slippage of neoprene bridge bearings, *Journal of Bridge Engineering*, *5(3)*, 216–223, https://doi.org/10.1061/(ASCE)1084-0702(2000)5:3(216)

[18] Pinarbasi, S. & Akyuz, U. (2004) Investigation of Compressive Stiffness of Elastomeric Bearings, *6th International Congress on Advances in Civil Engineering*, Bogazici University October 6–8, 2004, Istanbul, Turkey.

[19] Kumar, M. (2012) Analysis of Elastomeric Bearings in Compression. Unpublish Doctoral Dissertation, University at Buffalo, United State.

[20] Osgooei, P. M., Tait, M. J., & Konstantinidis, D. (2014) Three Dimensional Finite Element Analysis of Circular Fiber Reinforced Elastomeric Bearings Under Compression, *Composite Structure*, *108*, 191-204, https://doi.org/10.1016/j.compstruct.2013.09.008

[21] Imbimbo, M., & De Luca, A. (1998) F. E. Stress Analysis of Rubber Bearings Under Axial Loads, *Computers & Structures*, *68(1-3)*, 31-39, https://doi.org/10.1016/S0045-7949(98)00038-8

[22] Koo, G., Lee, J., Lee, H. & Yoo, B. (1999) Stability of Laminated Rubber Bearing and Its Application to Seismic Isolation, *KSME International Journal*, *13(8)*, 595-604, https://doi.org/10.1007/BF03184553

[23] Othman, A. (2001) Property Profile of a Laminated Rubber Bearing, *Polymer Testing*, *20(2)*, 159-166, https://doi.org/10.1016/S0142-9418(00)00017-9

[24] Chang, C. H. (2002) Modeling of Laminated Rubber Bearings Using an Analytical Stiffness Matrix, *International Journal of Solids and Structures*, *39(24)*, 6055-6078, https://doi.org/10.1016/S0020-7683(02)00471-7

[25] Kelly, J. M. & Marsico, M. R. (2013) Tension Buckling in Rubber Bearings Affected by Cavitation, *Engineering Structures*, *56*, 656-663, https://doi.org/10.1016/j.engstruct.2013.05.051

[26] Aloisio, A., Alaggio, R. & Fragiacomo, M. (2020) Dynamic identification and model updating of full-scale concrete box girders based on the experimental torsional response, *Construction and Building Materials*, *264*, 120146, https://doi.org/10.1016/j.conbuildmat.2020.120146

[27] Yusuf, A. I., Mohd Amin, N., Yunus, M. A. & Abdul Rani, M. N. (2018) Evaluation of Rayleigh Damping Coefficients for Laminated Rubber Bearing Components Using Finite Element and Experimental Modal Analysis, *International Journal of Integrated Engineering*, *10(9)*, 116–121, https://doi.org/10.30880/ijie.2018.10.09.004

[28] Yusuf, A. I., Amin, N. M., Yunus, M. A. & Rani, M. N. A. (2016) Dynamic properties of elastomeric bearing via finite element and experimental modal analysis, *Malaysian Construction Research Journal*, *19(2)*, 39-48

[29] Lin, R., & Lim, M. (1997) Modal analysis of close modes using perturbative sensitivity approach, *Engineering structures*, *19(6)*, 397-406, https://doi.org/10.1016/S0141-0296(96)00078-8

[30] Fu, Z.-F. & He, J. (2001) Modal analysis: Butterworth-Heinemann.

[31] Orlowitz, E. & Brandt, A. (2017) Comparison of experimental and operational modal analysis on a laboratory test plate, *Measurement*, *102*, 121–130, https://doi.org/10.1016/j.measurement.2017.02.001

[32] Kaewunruen, S & Remennikov, A. (2005) Application of experimental modal testing for estimating dynamic properties of structural components. *Australian Structural Engineering Conference 2005*, *2005*(ASEC), 11–14.

[33] Cusano, A. et al. (2006) Experimental modal analysis of an aircraft model wing by embedded fiber bragg grating sensors, *IEEE Sensors Journal*, *6(1)*, 67–77, https://doi.org/10.1109/JSEN.2005.854152

[34] Fouzi, M. S. M., Jelani, K. M., Nazri, N. A. & Sani, M. S. M. (2018) Finite Element Modelling and Updating of Welded Thin-Walled Beam, *International Journal of Automotive and Mechanical Engineering*, *15(4)*, 5874–5889, https://doi.org/10.15282/ijame.15.4.2018.12.0449

[35] Mohd Zin, M. S., Abdul Rani, M. N., Yunus, M. A., Wan Iskandar Mirza, W. I. I. & Sani, M. S. M. (2019) Experimental Modal Analysis Procedure for a Laser Spot Welded Hat Plate Structure, *Journal of Physics: Conference Series*, *1262*, 012015, https://doi.org/10.1088/1742-6596/1262/1/012015